

Online Data-Enabled Predictive Control

Stefanos Baros*, Chin-Yao Chang*, Gabriel E. Colón-Reyes, Andrey Bernstein

Abstract—We develop an online data-enabled predictive (ODeePC) control method for optimal control of unknown systems, building upon the recently proposed DeePC [23]. Our proposed ODeePC method leverages a primal-dual algorithm with real-time measurement feedback to iteratively compute the corresponding real-time optimal control policy as system conditions change. Specifically, our developed ODeePC: a) records data from the unknown system and updates the underlying primal-dual algorithm dynamically, b) can track changes in the system’s operating point and adjust the control inputs, and c) is computationally efficient as it deploys a Fast Fourier Transform-based algorithm enabling the fast computation of the product of a non-square Hankel matrix with a vector. We provide theoretical guarantees regarding the asymptotic behavior of ODeePC and demonstrate its performance through a power system application.

model, by capturing exogenous disturbances and other model details not accounted for in the existing model [21].

Recently, a data-enabled predictive control algorithm (DeePC) [23] has been proposed as an alternative approach that is free of any parametric system model representation. DeePC, rather, uses the control inputs and plant outputs of a dynamical system to learn the system’s behavior and compute a predictive control policy directly. Unfortunately, this control approach, despite its accuracy and efficacy for small systems (i.e., systems with few states), lacks scalability as its implementation to large systems (i.e., systems with many states) can be computationally burdensome. This is partially due to the large dataset required to accurately represent the underlying system.

Contributions. In this paper we develop an *online* data-enabled predictive controller (ODeePC) by building upon the recently proposed DeePC. Our main contributions are highlighted as follows.

- We appropriately design ODeePC so that it has the following properties: a) it can record data through measurements from the unknown system in real-time and update the underlying optimization problem accordingly; b) it can track changes in the system’s operating point and adjust the control inputs dynamically; and c) it is computationally efficient. The algorithm design leverages the online time-varying optimization methods with measurement feedback [28], [29].
- To enable online implementation of ODeePC, we devise a computationally efficient algorithm for a fast computation of the product of a non-square block Hankel matrix with a vector. The algorithm exploits properties of Circulant matrices and Fast Fourier Transforms to carry out the assigned computations efficiently. We also derive the complexity of this algorithm and prove that it precisely computes the desired product.
- Lastly, we establish theoretical guarantees regarding the asymptotic behavior of ODeePC and illustrate its effectiveness through numerical studies.

The rest of the paper is structured in the following way. In Section II, we present the notation we use throughout the paper and some preliminaries. In Section III, we review the classical MPC and the recently proposed DeePC [23]. Section IV includes the main results surrounding the development of the proposed ODeePC algorithm and analysis of its performance. We validate the performance of ODeePC through a numerical example in Section V. Finally, in Section VI, we conclude the paper with some remarks.

I. INTRODUCTION

In the context of smart critical infrastructures and complex dynamical systems, applications of optimal control abound [1]. Traditional optimal control of these systems relies on accurate system model, with model predictive control (MPC) [4]–[8] being a classic approach. However, many complex physical systems, such as large power systems, manifest complex and hard-to-model uncertain dynamics that complicate their study and analysis. Therefore, data-based modeling and control techniques have become increasingly popular in the context of such systems due to data abundance [2], [3]. Such approaches offer an attractive alternative to classic optimal control as they are independent of any analytical system models.

System identification algorithms are exploited in many control approaches for producing approximate models when an analytical system description might not be available or too difficult to obtain [18]–[20]. Other data-based control approaches exploit different types of learning algorithms at various stages of the control design process to generate information about the model. Representative publications of this line of work are [12]–[17], [21] and [22]; the most prominent approaches are based on reinforcement learning and MPC using Gaussian processes. All of these approaches rely on state-space model representation of the underlying dynamical system.

Data-driven optimal control approaches can be useful even in the case where a certain (simplified) model of the system exists. In such case, data-driven approaches can help refine the

Stefanos Baros, Chin-Yao Chang and Andrey Bernstein are with the National Renewable Energy Laboratory (NREL), {stefanos.baros, chinYao.chang, andrey.bernstein}@nrel.gov; Gabriel E. Colón-Reyes is with the Department of Electrical Engineering and Computer Science at the University of California, Berkeley, gecolonr@berkeley.edu. This work was authored in part by NREL, operated by Alliance for Sustainable Energy, LLC, for the U.S. Department of Energy (DOE) under Contract No. DE-AC36-08GO28308. Funding provided by DOE Office of Electricity, Advanced Grid Modeling Program, through agreement NO. 33652.

* The first two authors contributed equally.

II. NOTATION AND PRELIMINARIES

A. Notation

Let \mathbb{R} denotes the set of real numbers; $\mathbb{Z}_{\geq 0}$ and $\mathbb{Z}_{> 0}$ respectively denote the set of non-negative integers. Given a matrix A , A^\top denotes its transpose, $A \succ (\prec) 0$ denotes that A is positive (negative) definite. The matrix $I_n \in \mathbb{R}^{n \times n}$ is the $n \times n$ identity matrix. For $x \in \mathbb{R}^n$, $\|x\|_2$ denotes its Euclidean norm and $\text{diag}\{x\}$ is a diagonal matrix with the elements of x on the main diagonal. Given a $Q \succ 0$, we define $\|v\|_Q^2 = v^\top Q v$. We use subscript t to denote a vector value at time t ; and $v_{i,t}$ to denote the i^{th} entry of the vector v_t at time t . We denote the smallest eigenvalue of $Q \in \mathbb{R}^{n \times n}$ by $\lambda_{\min}(Q)$. A shift matrix is defined as $S_{m,n} = \begin{bmatrix} 0 & I_{m-1} \\ 0 & 0 \end{bmatrix} \otimes I_n$ and $S_{m,n} \in \mathbb{R}^{mn \times mn}$. For any matrix $A \in \mathbb{R}^{mn \times N}$, $S_{m,n} A$ results in shifting the elements of A upwards by n positions.

B. Preliminaries

Let us start by assuming that the system we seek to control can be represented by a discrete-time, linear, time-invariant (LTI) state-space model given by

$$\begin{cases} x_{t+1} = Ax_t + Bu_t \\ y_t = Cx_t + Du_t. \end{cases} \quad (1)$$

In this representation, $t \in \mathbb{Z}_{> 0}$ is the discrete time index; $A \in \mathbb{R}^{n \times n}$ is the state matrix; $B \in \mathbb{R}^{n \times m}$ is the input matrix; $C \in \mathbb{R}^{p \times n}$ is the output matrix; $D \in \mathbb{R}^{p \times m}$ is the feedforward matrix; $x_t \in \mathbb{R}^n$ is the state vector; $u_t \in \mathbb{R}^m$ is the control input vector; and $y_t \in \mathbb{R}^p$ is the output vector. Also, let $r_t \in \mathbb{R}^p$ denote the output *reference* vector representing the desired value of the output at time t .

Let $u := (u_1^\top, \dots, u_T^\top)^\top \in \mathbb{R}^{mT}$ denote the vector of the control inputs during $t = 1, \dots, T$, for some $T \in \mathbb{Z}_{> 0}$. The *block Hankel matrix* with each column being a set of consecutive data points of length $L \leq T$ is given by

$$\mathcal{H}_L(u) := \begin{bmatrix} u_1 & u_2 & \dots & u_{T-L+1} \\ u_2 & u_3 & \dots & u_{T-L+2} \\ \vdots & \vdots & \ddots & \vdots \\ u_L & u_{L+1} & \dots & u_T \end{bmatrix}, \quad (2)$$

with $\mathcal{H}_L(u) \in \mathbb{R}^{mL \times (T-L+1)}$. A similar matrix can be constructed for y .

It is useful at this point to introduce the following definition.

Definition II.1. Let $L, T \in \mathbb{Z}_{> 0}$ and $T \geq L$. Then, the signal $u := (u_1^\top, \dots, u_T^\top)^\top$ is persistently exciting of order L if $\mathcal{H}_L(u)$, as defined in (2), is of full row rank.

Roughly speaking, a persistently exciting input is a rich enough input able to excite the system so that it generates an output that is representative of its behavior.

Moving forward, let us assume that $u \in \mathbb{R}^{mT}$ is a persistently exciting input dataset of order T_{tot} . With rich enough data to describe system (1), we can construct the following Hankel matrices associated with the input and output data respectively

$$U := \mathcal{H}_{T_{\text{tot}}}(u), \quad Y := \mathcal{H}_{T_{\text{tot}}}(y), \quad (3)$$

where $U \in \mathbb{R}^{mT_{\text{tot}} \times \kappa}$, $Y \in \mathbb{R}^{pT_{\text{tot}} \times \kappa}$ and $\kappa := T - T_{\text{tot}} + 1$. Behavioral system theory [27] states that the input-output pair $(u_{\text{tot}}, y_{\text{tot}})$, where $u_{\text{tot}} \in \mathbb{R}^{mT_{\text{tot}}}$ and $y_{\text{tot}} \in \mathbb{R}^{pT_{\text{tot}}}$, is a trajectory of (1) if and only if there exists a $g \in \mathbb{R}^\kappa$ such that

$$\begin{bmatrix} U \\ Y \end{bmatrix} g = \begin{bmatrix} u_{\text{tot}} \\ y_{\text{tot}} \end{bmatrix}. \quad (4)$$

Equation (4) indicates that any possible trajectory should be a linear combination of κ number of trajectories (columns) embedded in $[U^\top, Y^\top]^\top$. We can view (4) as an alternative model of (1). The main difference is that (4) is entirely constructed by data as opposed to state evolution in (1).

III. OVERVIEW OF CLASSIC MPC AND DEEPC

In this section, we provide an overview of the classic MPC and the recently proposed DeePC [23]. We note that the classic MPC uses a precise model (1) while DeePC uses the recorded control inputs and plant outputs of the underlying system to capture its behavior and compute a predictive control policy.

A. MPC

MPC is a receding time horizon control algorithm that computes an optimal control input u_t based on a prediction of the system's future trajectory subject to the system's dynamics. We consider a classic MPC setting with prediction horizon $N \in \mathbb{Z}_{> 0}$ formulated as

$$\begin{aligned} & \underset{\substack{x, u_k \in \hat{U}, y_k \in \hat{Y}, \\ \forall k=0, \dots, N-1}}{\text{minimize}} && \sum_{k=0}^{N-1} f(u_k, y_k), && (5) \\ & \text{subject to} && x_{k+1} = Ax_k + Bu_k, \quad \forall k \in \{0, \dots, N-1\}, \\ & && y_k = Cx_k + Du_k, \quad \forall k \in \{0, \dots, N-1\}, \\ & && x_0 = \hat{x}_t, \end{aligned}$$

where $x = (x_0^\top, \dots, x_N^\top)^\top$, $\hat{U} \subseteq \mathbb{R}^m$ and $\hat{Y} \subseteq \mathbb{R}^p$ are respectively the convex constraint sets for u_k and y_k for all k , $f: \hat{U} \times \hat{Y} \mapsto \mathbb{R}$ is a convex cost function, and \hat{x}_t serves as the initial state of the system. A variable t is chosen to denote the current time and let k indexes the time instances of the look-ahead horizon window. Algorithm 1 [23] can be used to solve the MPC Problem (5). Usually, after the optimal

Algorithm 1 MPC [23]

Problem data: matrices A, B, C, D , current state \hat{x}_t , feasible input and output sets \hat{U} and \hat{Y} , objective function f .

- 1) Solve (5) for $u^* = (u_0^{*\top}, \dots, u_{N-1}^{*\top})^\top$.
 - 2) Apply inputs $(u_t^\top, \dots, u_{t+s}^\top)^\top = (u_0^{*\top}, \dots, u_s^{*\top})^\top$ for some $s \leq N-1$.
 - 3) Set t to $t+s$ and update \hat{x}_t .
 - 4) Repeat.
-

control policy is computed, only the input u_0^* that corresponds to the first look-ahead window is implemented to the system (or $s = 0$). In the rest of the paper, we will assume $s = 0$ without loss of generality.

The MPC algorithm described above has proven to be effective in numerous applications, e.g. autonomous driving

[9] and flight control [10], where the goal is primarily trajectory tracking. Despite that, the requirement for an accurate model description still restricts the application domain as systems whose dynamics are hard to model or unknown cannot be considered. To this end, DeePC, that leverages measured system data instead of an accurate system model to capture the system's behavior, overcomes the above limitations and has shown to work well for small systems. We review the DeePC control approach [23] next.

B. DeePC

DeePC relies on the past input/output data to construct the model shown in (4). Any input/output trajectory that is composed of the initial subtrajectory $(u_{\text{ini}}, y_{\text{ini}})$ and the subtrajectory $u = (u_0^\top, \dots, u_{N-1}^\top)^\top$ and $y = (y_0^\top, \dots, y_{N-1}^\top)^\top$, over the time interval t to $t + N - 1$, that we seek to compute, should be a linear combination of input/output trajectories previously obtained from data. In other words, a $g \in \mathbb{R}^\kappa$ should exist such that the following holds

$$\begin{bmatrix} U \\ Y \end{bmatrix} g = \begin{bmatrix} U_p \\ U_f \\ Y_p \\ Y_f \end{bmatrix} g = \begin{bmatrix} u_{\text{ini}} \\ u \\ y_{\text{ini}} \\ y \end{bmatrix}, \quad (6)$$

where $u_{\text{ini}} \in \mathbb{R}^{mT_{\text{ini}}}$ and $y_{\text{ini}} \in \mathbb{R}^{pT_{\text{ini}}}$ correspond to the input/output subtrajectory over the interval $(t - T_{\text{ini}}, \dots, t - 1)$, for some given $T_{\text{ini}} \in \mathbb{Z}_{>0}$, which is given. Further, we note that U and Y are obtained through measurements by observing the system for a total time T and arranging the input/output pairs in columns of length T_{tot} . Equation (6) is obtained from (4) by partitioning $U \in \mathbb{R}^{mT_{\text{tot}} \times \kappa}$ into U_p and U_f with $U_p \in \mathbb{R}^{mT_{\text{ini}} \times \kappa}$, $U_f \in \mathbb{R}^{m(N - T_{\text{ini}}) \times \kappa}$, where $T_{\text{tot}} = T_{\text{ini}} + N$. Similarly, $Y \in \mathbb{R}^{pT_{\text{tot}} \times \kappa}$ is partitioned into $Y_p \in \mathbb{R}^{pT_{\text{ini}} \times \kappa}$ and $Y_f \in \mathbb{R}^{p(N - T_{\text{ini}}) \times \kappa}$. Note that T_{ini} should be selected large enough to ensure unique y for any given u , cf. [27, Lemma 1]. We assume that the total number of measured input/output pairs, T , is large enough to construct a persistently exciting U . With the elements in place, we state the DeePC formulation of (5) as follows.

$$\underset{g \in \mathbb{R}^\kappa, u \in \mathcal{U}, y \in \mathcal{Y}}{\text{minimize}} \sum_{k=0}^{N-1} f(u_k, y_k) \text{ s.t. (6) holds,} \quad (7)$$

where \mathcal{U} and \mathcal{Y} are respectively the Cartesian products of N number of $\hat{\mathcal{U}}$ and $\hat{\mathcal{Y}}$. One can easily realize that, rather than having a discrete state-space representation of the system in place of the optimization problem's constraints, as is the case for MPC, here we have a set of linear equality constraints that are constructed using the input/output data samples. It follows that the relationship between the input u and the output y here is not imposed by a state-space model but by a linear equality constraint constructed from data. In [23], the following algorithm is proposed for solving Problem (7). We note that in the DeePC approach, the matrix $\mathcal{H} = [U_p^\top, U_f^\top, Y_p^\top, Y_f^\top]^\top$ is not updated over time as the data is recorded offline and used online to solve the receding horizon predictive control problem. Only the RHS elements $h = [u_{\text{ini}}^\top, u^\top, y_{\text{ini}}^\top, y^\top]^\top$ are

Algorithm 2 DeePC [23]

Problem data: past input data $u_{\text{ini}}, y_{\text{ini}}$, \mathcal{H} , feasible input and output sets \mathcal{U} and \mathcal{Y} , objective function f .

- 1) Solve (7) for g^* and compute $u^* = U_f g^*$.
 - 2) Apply control inputs $(u_t^\top, \dots, u_{t+s}^\top)^\top = (u_0^{*\top}, \dots, u_s^{*\top})^\top$ for some $s \leq N - 1$.
 - 3) Set t to $t + s$ and update past input/output data u_{ini} and y_{ini} with the T_{ini} most recent data obtained from measurements.
 - 4) Repeat.
-

updated as t evolves. In cases where we are dealing with time-varying or nonlinear systems, not updating the matrix \mathcal{H} over time may result in bad system representation and subsequently invalid computed control policies.

Next, we present our proposed Online Data-enabled Predictive Control (ODEePC) that has several advantages over the DeePC [23].

IV. ONLINE DATA-ENABLED PREDICTIVE CONTROL

The basic aspects of our proposed ODEePC can be highlighted as follows.

- It exploits available real-time data obtained from system measurements to dynamically update both the matrix \mathcal{H} and the vector h .
- It uses a primal-dual gradient descent algorithm to iteratively compute the optimal control policy, thus allowing the intermediate control inputs to be implemented to the system in real-time. Further, it allows real-time measured information about the system's state to take part in the algorithm and affect the computed optimal control policy.
- It exploits a Fast Fourier Transform-based algorithm to efficiently compute the products of block Hankel matrices with vectors.

The above aspects of ODEePC will be explained in detail.

A. Primal-dual Algorithm for the Regularized DeePC Problem

We first design a primal-dual algorithm to iteratively solve the regularized version of Problem (7). Then, we appropriately modify the designed algorithm in order to arrive at the ODEePC algorithm's iterative update rule. The regularized DeePC problem differs from the standard DeePC problem only in the choice of the objective function used. For completeness, we state the *regularized DeePC problem* here.

$$\underset{g \in \mathbb{R}^\kappa, u \in \mathcal{U}, y \in \mathcal{Y}}{\text{minimize}} \sum_{k=0}^{N-1} f(u_k, y_k) + \frac{\epsilon g}{2} \|g\|_2^2 \text{ s.t. (6) holds} \quad (8)$$

We use the method of Lagrange multipliers to solve the min-max optimization problem associated with Problem (8)

$$\underset{\nu}{\text{maximize}} \left(\underset{g \in \mathbb{R}^\kappa, u \in \mathcal{U}, y \in \mathcal{Y}}{\text{minimize}} \mathcal{L}(u, y, g, \nu) \right), \quad (9)$$

where $\nu \in \mathbb{R}^{N_\nu}$, $N_\nu = (m+p)(T_{\text{ini}} + N)$, and \mathcal{L} is the *regularized Lagrangian* given as:

$$\mathcal{L}(u, y, g, \nu) = \sum_{k=0}^{N-1} f(u_k, y_k) + \frac{\epsilon_g}{2} \|g\|_2^2 + \nu^\top (\mathcal{H}g - h) - \frac{\epsilon_\nu}{2} \|\nu\|_2^2.$$

The additional regularization terms improve the convergence rate of the gradient-based method at the expense of converging to a point that is close to but not exactly the real optimal point of (8). This particular regularization is widely used for solving convex optimization problems [28], [29]. Using the primal-dual gradient descent algorithm to solve (9), we arrive at the problem's saddle-flow dynamics. These, are given by

$$u^{\tau+1} = \text{Proj}_{\mathcal{U}}\{u^\tau - \alpha(\nabla_u \tilde{f}|_{(u^\tau, y^\tau)} - \nu_u^\tau)\}, \quad (10a)$$

$$y^{\tau+1} = \text{Proj}_{\mathcal{Y}}\{y^\tau - \alpha(\nabla_y \tilde{f}|_{(u^\tau, y^\tau)} - \nu_y^\tau)\}, \quad (10b)$$

$$g^{\tau+1} = g^\tau - \alpha(\mathcal{H}^\top \nu^\tau + \epsilon_g g^\tau), \quad (10c)$$

$$\nu^{\tau+1} = \nu^\tau + \alpha(\mathcal{H}g^\tau - h - \epsilon_\nu \nu^\tau), \quad (10d)$$

where τ is the iteration number, $\alpha \in \mathbb{R}_+$ is the step size, and $\tilde{f} := [f(u_0, y_0), \dots, f(u_{N-1}, y_{N-1})]^\top$. Further, $\text{Proj}_{\mathcal{X}}\{x\}$ denotes projection of x onto the constraint set \mathcal{X} . Further, we define ν_u^τ and ν_y^τ as the elements of ν^τ associated with the inputs and outputs, respectively. The saddle-flow dynamics (10) solve the *static* optimization problem (8).

Relatively large systems with numerous states would give rise to a large matrix \mathcal{H} . This would inevitably render the above algorithm computationally very expensive. To see this consider that the product of a general matrix $\mathcal{H} \in \mathbb{R}^{n \times m}$ with a m -element vector (at every iteration as imposed by (10c) and (10d)), can be computed by carrying out $n \times m$ multiplications and $(n \times m - n)$ additions. One can realize that exact and real-time computation of this product and thus implementation of the above algorithm would be quite challenging. This would be even more challenging in an online setting where, u_{ini} , y_{ini} and \mathcal{H} would be frequently updated. Motivated by this, we carefully design ODDePC so that it is computationally efficient and practically implementable. We accomplish this by exploiting a computationally efficient algorithm that leverages Fast Fourier Transforms (FFT) to compute the block Hankel matrix-vector multiplication fast. The details will be provided in the sequel.

B. ODDePC

We are now ready to present the underlying time-varying optimization problem associated with our proposed ODDePC. We consider, the vector h in the optimization (7) to be frequently updated with the latest input-output pair u_{ini} and y_{ini} . In addition, to allow our algorithm to cope with time-varying systems, we also update \mathcal{H} at every iteration for better

system characterization. The following formulation captures the time-varying properties described above.

$$\begin{aligned} & \underset{g \in \mathbb{R}^n, u \in \mathcal{U}, y \in \mathcal{Y}}{\text{minimize}} && \sum_{k=0}^{N-1} f(u_k, y_k) + \frac{\epsilon_g}{2} \|g\|_2^2, \\ & \text{subject to} && \begin{bmatrix} U_p^t \\ U_f^t \\ Y_p^t \\ Y_f^t \end{bmatrix} g = \begin{bmatrix} u_{\text{ini}}^t \\ u \\ y_{\text{ini}}^t \\ y \end{bmatrix}, \end{aligned} \quad (11)$$

where t captures the time instances when the optimization problem is updated.

Remark IV.1. (ODDePC for linear time-varying (LTV) systems). For a LTI system, updating \mathcal{H} online using the measured data is not very meaningful as the original \mathcal{H} already captures all the properties that characterize the system. However, in allowing ODDePC to deal with LTV systems or nonlinear dynamical systems, frequent online updating of the matrix \mathcal{H} becomes critical.

Let the variable τ track the algorithm iteration and assume that the control is implemented on the system every time N_I iterations have been completed. The iteration index τ and the system update instances t are related as follows. When τ coincides with system update instant t , then $\tau + N_I$ would coincide with the system update instant $t + 1$. In our proposed ODDePC system, all the inner-loop iterations in the interval $(t, t + 1)$ are carried out using the update rules (10) with \mathcal{H} being fixed and given by $\mathcal{H}^t = [U_p^{t\top} \ U_f^{t\top} \ Y_p^{t\top} \ Y_f^{t\top}]^\top$. In addition, u_{ini} and y_{ini} elements of h are respectively fixed at u_{ini}^t and y_{ini}^t . However, every N_I iterations, starting at instant $t + 1$ (or $\tau + N_I$), these elements are updated and ODDePC deploys the following update rules to compute the new input-output pairs and dual variables

$$u^{\tau+1} = \text{Proj}_{\mathcal{U}}\{\hat{u}^\tau - \alpha(\nabla_u \tilde{f}|_{(\hat{u}^\tau, \hat{y}^\tau)} - \hat{\nu}_u^\tau)\}, \quad (12a)$$

$$y^{\tau+1} = \text{Proj}_{\mathcal{Y}}\{\hat{y}^\tau - \alpha(\nabla_y \tilde{f}|_{(\hat{u}^\tau, \hat{y}^\tau)} - \hat{\nu}_y^\tau)\}, \quad (12b)$$

$$g^{\tau+1} = g^\tau - \alpha(\mathcal{H}^{(t+1)\top} \hat{\nu}^\tau + \epsilon_g g^\tau), \quad (12c)$$

$$\nu^{\tau+1} = \hat{\nu}^\tau + \alpha(\mathcal{H}^{t+1} g^\tau - h^{t+1} - \epsilon_\nu \hat{\nu}^\tau), \quad (12d)$$

where $\hat{u}^\tau = S_{N,m} u^\tau$, $\hat{y}^\tau = S_{N,p} y^\tau$, $\hat{\nu}^\tau = [\hat{\nu}_u^\tau \ \hat{\nu}_y^\tau]^\top$, $\hat{\nu}_u^\tau = S_{T_{\text{tot}},m} \nu_u^\tau$, $\hat{\nu}_y^\tau = S_{T_{\text{tot}},p} \nu_y^\tau$. Observe that the update rules (12) are different from (10). The main differences between (12) and (10) are that the variables u^τ , y^τ , ν^τ are updated through the shift matrices and the Hankel matrix \mathcal{H} and vector h are also updated. The shift matrix moves u_{k+1}^τ in the place of u_k^τ for all $k = 0, \dots, N - 2$. The other variables are updated similarly through the shift matrices. The logic behind this updating scheme is that the prediction horizon changes, e.g from $(t, t + 1, \dots, t + N - 1)$ to $(t + 1, t + 2, \dots, t + N)$, every time the optimization problem is getting updated. The updating scheme uses the shift matrices to appropriately “initialize” the solution of the optimization problem at $t + 1$ using the one for time t . We summarize the ODDePC in Algorithm 3.

Algorithm 3 Online Data-enabled Predictive Control (ODePC)

1: **Initialize** $\tau = t = 1, \alpha, \epsilon, u^\tau, y^\tau, g^\tau, \nu^\tau, \mathcal{H}^t, h^t$
 2: **Repeat**
 3: **if** $\text{mod}(\tau, N_I) \geq 1$ **then**
 4: Compute (10) using Algorithm 5
 5: **else**
 6: Apply control u_0^τ to the system
 7: Update \mathcal{H}^{t+1} and h^{t+1} using new u_0^τ and y_0^τ
 8: Compute (12) using Algorithm 5
 9: $t \mapsto t + 1$
 10: **end if**
 11: $\tau \mapsto \tau + 1$

Note that Algorithm 3 incorporates Algorithm 5, which will be introduced in section IV-D, to compute $\mathcal{H}^{\tau^\top} \nu^\tau$ and $\mathcal{H}^\tau g^\tau$ in (10) and (12). The matrix-vector multiplications are the most computationally heavy part in Algorithm 3. Algorithm 5 gets around the multiplications with Fast Fourier Transforms (FFT). We will first show the convergence of the ODePC in the next section and then explain how FFT-based approach works in section IV-D.

C. Convergence of ODePC

In this section, we will show that under mild assumptions, Algorithm 3 converges Q-linearly to a neighborhood of the optimal point. For convenience of notation, we denote $z^\tau = [u^{\tau^\top} y^{\tau^\top} g^{\tau^\top} \nu^{\tau^\top}]^\top$ and rewrite (12) as

$$z^{\tau+1} = \text{Proj}_{\mathcal{U} \times \mathcal{Y} \times \mathbb{R}^{\kappa+N_\nu}} \{z^\tau - \alpha \Psi^\tau(z^\tau)\}, \quad (13)$$

where the time-varying gradient step is embedded in Ψ^τ . We assume the Lipschitz continuity and monotonicity of Ψ^τ , stated formally in Assumption 1.

Assumption 1. (Lipschitz continuity and monotonicity of the gradient). *There exists a finite constant $\sigma_\Psi \in \mathbb{R}_+$ such that $\|\Psi^\tau(z^1) - \Psi^\tau(z^2)\| \leq \sigma_\Psi \|z^1 - z^2\|$ for all $z^1, z^2 \in \mathcal{U} \times \mathcal{Y} \times \mathbb{R}^{\kappa+N_\nu}$ for all τ . In addition, Ψ^τ is strongly monotone with constant η .*

As we have added the regularization terms in (10) and (12), Assumption 1 follows if we constrain g in a bounded and closed convex set and $\|H^t\|_2$ is finite for all t , c.f. [30, Lemma 3.4]. The reason of making Assumption 1 instead of deriving [30, Lemma 3.4] by adding those assumptions is that the proof of [30, Lemma 3.4] will require breaking the equality constraint on g into inequality constraints and separating discussions on (10) and (12), which are tedious and not the focus of this paper. We further make Assumption 2 that considers that the variation of the optimal point is bounded, enabling each time close tracking of the optimal point within a reasonable number of iterations of ODePC.

Assumption 2. (Bounded variation of the optimal point). *There exists a finite constant $\sigma_z \in \mathbb{R}_+$ such that the optimal points for the consecutive time steps t (or τ) and $t + 1$ (or $\tau + N_I$) of optimization (11) satisfy $\|z^{\tau+N_I, \star} - z^{\tau, \star}\|_2 \leq \sigma_z$.*

Recall that we index z by the iteration number rather than the time instances t . The optimal point of z for iterations $\tau, \dots, \tau + N_I - 1$ (or time t) stays unchanged because the associated optimization remains the same. The optimal point changes for iteration $\tau + N_I$ (time $t + 1$). With all the elements in place, we state Theorem IV.2 that establishes convergence of Algorithm 3.

Theorem IV.2. (Convergence of ODePC).¹ *If Assumptions 1 and 2 hold, and $\rho(\alpha) := \sqrt{1 + \alpha^2 \sigma_\Psi^2} - 2\alpha\eta < 1$, then Algorithm 3 has z^τ converge Q-linearly to a neighborhood of optimal point of (11), given as*

$$\limsup_{\tau \rightarrow \infty} \|z^\tau - z^{\tau, \star}\|_2 = \frac{\sigma_z}{1 - \rho(\alpha)}.$$

Proof. We first derive the inequality that includes $\|z^\tau - z^{\tau, \star}\|$ and $\|z^{\tau+1} - z^{\tau+1, \star}\|_2$ by considering $\|z^{\tau+1} - z^{\tau, \star}\|_2$ with the following algebra

$$\begin{aligned} \|z^{\tau+1} - z^{\tau, \star}\|_2 &= \|\text{Proj}_{\mathcal{U} \times \mathcal{Y} \times \mathbb{R}^{\kappa+N_\nu}} \{z^\tau - \alpha \Psi^\tau(z^\tau)\} - z^{\tau, \star}\|_2 \\ &= \|\text{Proj}_{\mathcal{U} \times \mathcal{Y} \times \mathbb{R}^{\kappa+N_\nu}} \{z^\tau - \alpha \Psi^\tau(z^\tau)\} \\ &\quad - \text{Proj}_{\mathcal{U} \times \mathcal{Y} \times \mathbb{R}^{\kappa+N_\nu}} \{z^{\tau, \star} - \alpha \Psi^\tau(z^{\tau, \star})\}\|_2 \\ &\leq \|z^\tau - \alpha \Psi^\tau(z^\tau) - z^{\tau, \star} + \alpha \Psi^\tau(z^{\tau, \star})\|_2. \end{aligned} \quad (14)$$

The first equality of (14) is due to (13); the second equality is by the fact that $z^{\tau, \star}$ is a fixed point of (13). The inequality of (14) is from non-expansivity of the projection.

By Assumption 1, the following inequalities hold

$$\eta \|z^\tau - z^{\tau, \star}\|_2^2 \leq \left(\Psi^\tau(z^\tau) - \Psi^\tau(z^{\tau, \star}) \right)^\top \left(z^\tau - z^{\tau, \star} \right), \quad (15a)$$

$$\|\Psi^\tau(z^\tau) - \Psi^\tau(z^{\tau, \star})\|_2^2 \leq \sigma_\Psi^2 \|z^\tau - z^{\tau, \star}\|_2^2. \quad (15b)$$

Combining (14) and (15) gives

$$\|z^{\tau+1} - z^{\tau, \star}\|_2 \leq \sqrt{1 + \alpha^2 \sigma_\Psi^2 - 2\alpha\eta} \|z^\tau - z^{\tau, \star}\|_2. \quad (16)$$

We further use Assumption 2 on the inequality above,

$$\|z^{\tau+1} - z^{\tau+1, \star}\|_2 \leq \rho(\alpha) \|z^\tau - z^{\tau, \star}\|_2 + \sigma_z. \quad (17)$$

If $\rho(\alpha) < 1$, then (17) is a contraction, which gives

$$\|z^{\tau+1} - z^{\tau+1, \star}\|_2 \leq \rho^\tau(\alpha) \|z^0 - z^{0, \star}\|_2 + \frac{1 - \rho^\tau(\alpha)}{1 - \rho(\alpha)} \sigma_z.$$

The term $\rho^\tau(\alpha) \|z^0 - z^{0, \star}\|_2 \rightarrow 0$ as $\tau \rightarrow \infty$, which completes the proof. \square

D. Fast Computation of Hankel Matrix-vector Product

In this section, we describe Algorithm 5 that computes the matrix-vector multiplications in (10) and (12) efficiently. We will use the fact that \mathcal{H} in (10) and (12) is the concatenation of block Hankel matrices U and Y , and apply FFT to exploit the convolutional structure of the Hankel matrices.

We slightly abuse the notation in this subsection and let n and m denote the dimensions of a general Hankel matrix \mathbf{H} so that $\mathbf{H} \in \mathbb{R}^{n \times m}$, unrelated to the state-space model

¹We assume the measurement noise is zero in the proof.

representation (1). Given that, the main problem we are concerned with here can be described as follows.

Problem 1. Given a m -element vector $v \in \mathbb{R}^m$

$$v := (v_1 \ v_2 \ \cdots \ v_m)^\top, \quad (18)$$

and a Hankel matrix $\mathbf{H} \in \mathbb{R}^{n \times m}$ where $h_i \in \mathbb{R}$, $\forall i$, defined as

$$\mathbf{H} := \begin{pmatrix} h_1 & h_2 & \cdots & h_{m-1} & h_m \\ h_2 & h_3 & \cdots & h_m & h_{m+1} \\ \vdots & \vdots & & & \\ h_{n-1} & h_n & \cdots & h_{n+m-3} & h_{n+m-2} \\ h_n & h_{n+1} & \cdots & h_{n+m-2} & h_{n+m-1} \end{pmatrix}, \quad (19)$$

compute the product $p_H = \mathbf{H}v$ in a computationally efficient manner.

Building upon the algorithm proposed in [26] for computing the product of a square Hankel matrix and a vector, we propose Algorithm 4 for computing the product $p_H = \mathbf{H}v$ efficiently for *non-square Hankel matrices*. The complexity of Algorithm 4 is introduced through the following theorem.

Algorithm 4 Fast Hankel matrix-vector product

Given a vector $v \in \mathbb{R}^m$ and a Hankel matrix $\mathbf{H} \in \mathbb{R}^{n \times m}$, compute the vector $p_H = \mathbf{H}v$ via the following steps.

- 1) Define a new $(n + m - 1)$ -element vector c as:

$$c = (h_m \ h_{m+1} \ \cdots \ h_{n+m-1} \ h_1 \ h_2 \ \cdots \ h_{m-1})^\top$$

We note that the vector c is the vector that fully specifies a Circulant matrix \mathbf{C} .

- 2) Define a $(n + m - 1)$ -element vector $v_e \in \mathbb{R}^{n+m-1}$ by permuting the vector v and adding $(n - 1)$ zeros so that:

$$v_e = (v_m \ v_{m-1} \ \cdots \ v_1 \ 0 \ \cdots \ 0)^\top$$

- 3) Compute a $(n + m - 1)$ -element vector y as:

$$y = \mathbf{IFFT}(\mathbf{FFT}(c) \circ \mathbf{FFT}(v_e))$$

where (\circ) is the Hadamard product of the two vectors, \mathbf{FFT} the Fast Fourier Transform and \mathbf{IFFT} the inverse Fast Fourier Transform.

- 4) Let $y = (y_1 \ y_2 \ \cdots \ y_{(n+m-2)} \ y_{(n+m-1)})^\top$, $y \in \mathbb{R}^{n+m-1}$. Then the product $p_H = \mathbf{H}v$ is given by:

$$p_H = (y_1 \ y_2 \ \cdots \ y_{n-1} \ y_n)^\top$$

i.e the subvector defined by the first n elements of the vector y .

Theorem IV.3. The complexity of Algorithm 4 that computes the product of a Hankel matrix $\mathbf{H} \in \mathbb{R}^{n \times m}$ and a vector $v \in \mathbb{R}^m$ is $O(\max(n, m) \log(\max(n, m)))$.

Proof. Following the same steps as in [26], we first note that each of the FFT has a complexity $5(n + m - 1) \log(n + m - 1)$, the pointwise multiplication has a complexity $6(n + m - 1)$ and the inverse FFT $5(n + m - 1) \log(n + m - 1)$. By combining all

these together, we have that the complexity of the algorithm is

$$15(n + m - 1) \log(n + m - 1) + 6(n + m - 1). \quad (20)$$

Equation (20) can be rewritten in Big-O notation, which is the desired $O(\max(n, m) \log(\max(n, m)))$. \square

It remains to show that the proposed algorithm precisely computes the desired product $p_H = \mathbf{H}v$. This is carried out through the following theorem.

Theorem IV.4. Consider a Hankel matrix $\mathbf{H} \in \mathbb{R}^{n \times m}$ as defined in (19) and a vector $v \in \mathbb{R}^m$ as defined in (18). The first n elements of the vector y obtained from the following computation

$$y = \mathbf{IFFT}(\mathbf{FFT}(c) \circ \mathbf{FFT}(v_e)) \quad (21)$$

where c and v_e are $(n + m - 1)$ -element vectors defined as

$$c := (h_m \ h_{m+1} \ \cdots \ h_{n+m-1} \ h_1 \ h_2 \ \cdots \ h_{m-1})^\top, \\ v_e := (v_m \ v_{m-1} \ \cdots \ v_1 \ 0 \ \cdots \ 0)^\top,$$

yields the exact product $p_H = \mathbf{H}v$.

Proof. The proof is deferred to the Appendix. \square

Through the above theorem, we have established that Algorithm 4 computes indeed the product $p_H = \mathbf{H}v$. By building upon the above results we will now design an algorithm that will allow us to compute efficiently the product of a *block* Hankel matrix \mathbf{H} (composed of column vectors \mathbf{h}_i) and a vector v . The main problem we seek to address can be stated as follows.

Problem 2. Given a m -element vector $v \in \mathbb{R}^m$

$$v := (v_1 \ v_2 \ \cdots \ v_m)^\top, \quad (22)$$

and a block Hankel matrix $\mathbf{H} \in \mathbb{R}^{(nl) \times m}$ where $\mathbf{h}_i \in \mathbb{R}^l$, $l > 1$, $\forall i$, defined as

$$\mathbf{H} := \begin{pmatrix} \mathbf{h}_1 & \mathbf{h}_2 & \cdots & \mathbf{h}_{m-1} & \mathbf{h}_m \\ \mathbf{h}_2 & \mathbf{h}_3 & \cdots & \mathbf{h}_m & \mathbf{h}_{m+1} \\ \vdots & \vdots & & & \\ \mathbf{h}_{n-1} & \mathbf{h}_n & \cdots & \mathbf{h}_{n+m-3} & \mathbf{h}_{n+m-2} \\ \mathbf{h}_n & \mathbf{h}_{n+1} & \cdots & \mathbf{h}_{n+m-2} & \mathbf{h}_{n+m-1} \end{pmatrix}, \quad (23)$$

Compute the product $p_{BH} = \mathbf{H}v$ in a computationally efficient manner.

Our goal here is to compute the product of a block Hankel matrix \mathbf{H} that is comprised of column vectors $\mathbf{h}_i \in \mathbb{R}^l$, with a vector v . We propose the following algorithm for solving Problem (2).

Following the steps in the proof of Theorem IV.4, one can show that application of Algorithm 5 indeed results in the precise computation of the product p_{BH} of a block Hankel matrix \mathbf{H} and a vector v .

Algorithm 5 Fast block Hankel matrix - vector product

The product p_{BH} of a vector $v \in \mathbb{R}^m$ and a block Hankel matrix $\mathbf{H} \in \mathbb{R}^{(nl) \times m}$ can be computed through the following steps.

- 1) **Initialize** $\beta = 1$ and define the vector $c \in \mathbb{R}^{l(n+m-1)}$

$$c = (\mathbf{h}_m^\top \ \cdots \ \mathbf{h}_{n+m-1}^\top \ \mathbf{h}_1^\top \ \mathbf{h}_2^\top \ \cdots \ \mathbf{h}_{m-1}^\top)^\top$$

- 2) Define a $(n+m-1)$ -element vector $v_e \in \mathbb{R}^{n+m-1}$ by permuting the vector v and adding $(n-1)$ zeros so that

$$v_e = (v_m \ v_{m-1} \ \cdots \ v_1 \ 0 \ \cdots \ 0)^\top$$

- 3) While $\beta \leq l$, construct

$$c^{(\beta)} = (\mathbf{h}_m(\beta) \ \cdots \ \mathbf{h}_{n+m-1}(\beta) \ \mathbf{h}_1(\beta) \ \cdots \ \mathbf{h}_{m-1}(\beta))^\top$$

and apply **Algorithm 4**, where $c = c^{(\beta)}$, to obtain $y^{(\beta)} = y \in \mathbb{R}^{n+m-1}$. Update $\beta \rightarrow \beta + 1$.

- 4) Compute the product $p_{\text{BH}} = \mathbf{H}v \in \mathbb{R}^{nl}$ a

$$p_{\text{BH}} = (y^{(1)}(1) \ \cdots \ y^{(l)}(1) \ \cdots \ y^{(1)}(n) \ \cdots \ y^{(l)}(n))^\top$$

V. NUMERICAL VALIDATION OF ODEEPC

We consider the following predictive control problem with a linear time-varying dynamical system

$$\begin{aligned} & \underset{x, u \in \mathcal{U}, y \in \mathcal{Y}}{\text{minimize}} && \sum_{k=0}^{N-1} \|y_k - r_{t+k}\|^2 && (24) \\ & \text{subject to} && x_{k+1} = A_k x_k + B_k u_k, \forall k \in \{0, \dots, N-1\}, \\ & && y_k = C x_k, \forall k \in \{0, \dots, N-1\} \\ & && x_0 = \hat{x}_t \end{aligned}$$

where $A_t \in \mathbb{R}^{10 \times 10}$, $B_t \in \mathbb{R}^{10 \times 10}$, $C \in \mathbb{R}^{10 \times 10}$, and r_t is the reference signal. The references r_t are changed randomly with uniform distribution between $[0, 0.1]$ for every 1000 iterations of t . To apply DeePC or ODeePC to the predictive control problem defined by (24), we construct the data-based model (6) by pre-running a number of iterations with a sequence of u_t which is persistently exciting of order $10(T_{\text{ini}} + N)$. Optimization (24) can then be reformulated in the form of (11) (the objective function can be time-varying without loss of generality). The parameters of the optimization and model are given in Table I.

N_I	T_{ini}	N	κ	ϵ_g
50	20	1800	1651	0.1

TABLE I: Number setup for the simulations.

After setting up the optimization, we run both DeePC and ODeePC with A_t and B_t being changed for every t . Specifically, the magnitude of each entry of A_t increases $p\%$ of its value whenever t changes to $t+1$, where p is randomly generated with a uniformly distribution in $[-0.01, 0.01]$. Similar biases are imposed to B_t . With these biases, the optimization associated with DeePC becomes infeasible in only less than 10 iterations. For comparison purposes, we run Gradient-DeePC which is the same as Algorithm 3 except that H^t is kept

unchanged over time. The biased variations of A_t and B_t also explains what we observe in Figures 1 and 2 that Gradient-DeePC starts diverging at around $t = 6000$. On the contrary, the ODeePC algorithm converges to a near optimal point with the cost close to zero.

Another reason for the performance difference between ODeePC and Gradient-DeePC is on the element shifting step embedded in (12) when the optimization is updated from t to $t+1$. Recall that ODeePC updates both H and h while Gradient-DeePC updates h and keeps H unchanged. This makes a difference as the shifting on variable z results in proper initialization of the optimization problem at $t+1$ using the solution at t . For the case of ODeePC, the majority of the constraints defined by $Hg = h$ are kept when t is changed to $t+1$, so the shifts defined in (12) result in variables that satisfy most of the equality constraints of the optimization problem at $t+1$. On the contrary, Gradient-DeePC only shifts h when the optimization problem is updated. This implies all the constraints of the optimization problem at $t+1$ are different from the ones at t . The ‘‘disconnection’’ between consecutive instances of the optimization problem is an additional disadvantage of Gradient-DeePC compared to ODeePC, which partially causes the divergence observed in Figure 3.

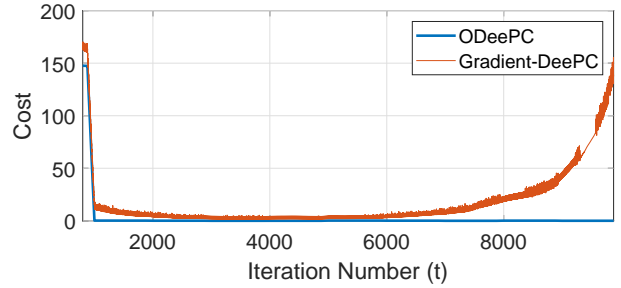


Fig. 1: Evolution of costs over iterations for ODeePC and Gradient-DeePC algorithms.

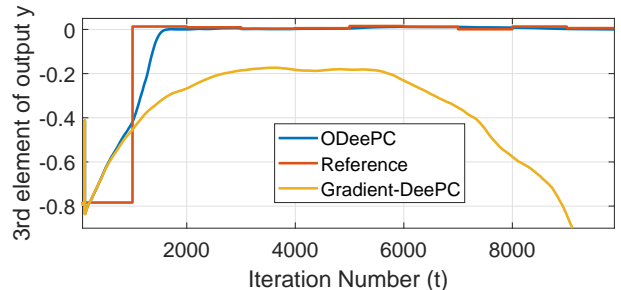


Fig. 2: Tracking performance of one entry of the output y .

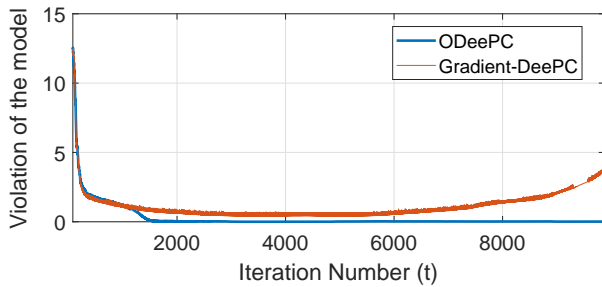


Fig. 3: Two norm violation of equality (6).

We also compare the computational times between Algorithm 5 and the direct matrix vector multiplication method. In our rather moderate-scale example, Algorithm 5 takes 0.51 seconds on average with $N_I = 50$ inner gradient iterations, while the average time for the direct multiplication is around 1.1 seconds. Both simulations are done on a desktop with 3.5GHz CPU and 16GB RAM. Algorithm 5 slashes the computational time in half and the advantage expands for larger scale systems.

VI. CONCLUSIONS AND FUTURE WORK

In this paper, we presented an online data-enabled predictive (ODeePC) control method for optimal control of unknown systems, building upon the recently proposed DeePC [23]. Our proposed ODeePC method leverages a primal-dual algorithm with real-time measurement feedback and recorded system data to compute the optimal control policy in real-time as system conditions change. ODeePC can generate control inputs dynamically, tracking changes in the system operating point while manifesting high computational efficiency. We prove that ODeePC's iterative update rule converges to a neighborhood of the optimal control policy. In future work, we would like to explore ways to leverage information about the physical laws that govern the dynamics of the system in our data-driven method, in order to construct a more reliable system model and thus have a more robust overall control method.

REFERENCES

- [1] A. M. Annaswamy, A. Malekpour, S. Baros, "Emerging research topics in control for smart infrastructures", *Annual Reviews in Control*, Volume 42, 2016, Pages 259-270.
- [2] F. Lamnabhi-Lagarigue, A. Annaswamy, S. Engell, A. Isaksson, P. Khargonekar, R.M. Murray, H. Nijmeijer, T. Samad, D. Tilbury, and P. Van den Hof, "Systems & Control for the future of humanity, research agenda: Current and future roles, impact and grand challenges", *Annual Reviews in Control*, Vol. 43, pp. 1-64, 2017.
- [3] Z. S. Hou and Z. Wang, "From model-based control to data-driven control: Survey, classification and perspective", *Information Sciences*, Vol. 235, pp.3-35, 2013.
- [4] J. B. Rawlings and D. Q. Mayne, "Model Predictive Control: Theory and Design", *Nob Hill Publishing*, 2009.
- [5] E. F. Camacho and C. B. Alba, "Model Predictive Control", *Springer Science & Business Media*, 2013.
- [6] A. Bemporad and M. Morari, "Robust model predictive control: A survey," in *Robustness in identification and control*, Springer, 1999, pp. 207-226.
- [7] D. Q. Mayne, "Model predictive control: Recent developments and future promise." *Automatica*, vol. 50, no. 12, pp. 2967-2986, 2014.
- [8] F. Borrelli, A. Bemporad, and M. Morari, "Predictive Control for Linear and Hybrid Systems", *Cambridge University Press*, 2017.

- [9] M. Brown, J. Funke, S. Erlien, and J. C. Gerdes, "Safe driving envelopes for path tracking in autonomous vehicles," *Control Engineering Practice*, vol. 61, pp. 3073-16, 2017.
- [10] I. Prodan, S. Oлару, R. Bencatel, J. B. de Sousa, C. Stoica, and S.-I. Niculescu, "Receding horizon flight control for trajectory tracking of autonomous aerial vehicles," *Control Engineering Practice*, vol. 21, no. 10, pp. 1334-1349, 2013.
- [11] G. Darivianakis, A. Georghiou, R. S. Smith, and J. Lygeros, "The power of diversity: Data-driven robust predictive control for energy efficient buildings and districts," *IEEE Transactions on Control Systems Technology*, 2017.
- [12] F. L. Lewis, D. Vrabie, and K. G. Vamvoudakis, "Reinforcement learning and feedback control: Using natural decision methods to design optimal adaptive controllers," *IEEE Control Systems*, vol. 32, no. 6, pp. 76-105, 2012.
- [13] Y. Ouyang, M. Gagrani, and R. Jain, "Learning-based control of unknown linear systems with Thompson sampling," *arXiv preprint*, arXiv:1709.04047, 2017.
- [14] B. Kiumarsi, F. L. Lewis, H. Modares, A. Karimpour, and M.-B. Naghibi-Sistani, "Reinforcement Q-learning for optimal tracking control of linear discrete-time systems with unknown dynamics," *Automatica*, vol. 50, no. 4, pp. 1167-1175, 2014.
- [15] A. M. Devraj and S. Meyn, "Zap Q-learning," in *Advances in Neural Information Processing Systems*, 2017, pp. 2235-2244.
- [16] B. Recht, "A tour of reinforcement learning: The view from continuous control," *arXiv preprint*, arXiv:1806.09460, 2018.
- [17] R. Islam, P. Henderson, M. Gomrokchi, and D. Precup, "Reproducibility of benchmarked deep reinforcement learning tasks for continuous control," *arXiv preprint*, arXiv:1708.04133, 2017.
- [18] M. C. Campi and E. Weyer, "Finite sample properties of system identification methods," *IEEE Transactions on Automatic Control*, vol. 47, no. 8, pp. 1329-1334, 2002.
- [19] M. Vidyasagar and R. L. Karandikar, "A learning theory approach to system identification and stochastic adaptive control," in *Probabilistic and randomized methods for design under uncertainty*. Springer, 2006, pp. 265-302.
- [20] S. Tu, R. Boczar, A. Packard, and B. Recht, "Non-asymptotic analysis of robust control from coarse-grained identification," *arXiv preprint*, arXiv:1707.04791, 2017.
- [21] F. Berkenkamp, M. Turchetta, A. Schoellig, and A. Krause, "Safe model-based reinforcement learning with stability guarantees," in *Advances in Neural Information Processing Systems*, 2017, pp. 908-918.
- [22] J. F. Fisac, A. K. Akametalu, M. N. Zeilinger, S. Kaynama, J. Gillula, and C. J. Tomlin, "A general safety framework for learning-based control in uncertain robotic systems," *IEEE Transactions on Automatic Control*, 2018.
- [23] J. Coulson, J. Lygeros and F. Dorfler, "Data-Enabled Predictive Control: In the Shallows of the DeePC", *18th European Control Conference (ECC)*, Napoli, Italy, June 25-28, 2019
- [24] A. Townsend, "Matrix-vector multiplication using the FFT", *Math, MIT, Notes*, 2015
- [25] G. Beliakov, "On fast matrix-vector multiplication with a Hankel matrix in multiprecision arithmetics", *arXiv preprint*, arXiv:1402.5287v2, 2014.
- [26] F. T. Luk and S. Qiao, "A fast eigenvalue algorithm for Hankel matrices," *Linear Algebra and its Applications*, 316:171-182, 2000.
- [27] I. Markovskiy and P. Rapisarda, "Data-driven simulation and control," *International Journal of Control*, vol. 81, no. 12, pp. 1946-1959, 2008.
- [28] A. Bernstein, E. Dall'Anese and A. Simonetto, "Online Primal-Dual Methods With Measurement Feedback for Time-Varying Convex Optimization," *IEEE Transactions on Signal Processing*, Vol. 67, No. 8, April 1, 2019
- [29] A. Bernstein and E. Dall'Anese, "Real-time Feedback-Based Optimization of Distribution Grids: A Unified Approach," *IEEE Transactions on Control of Network Systems*, Vol. 6, No. 3, September, 2019
- [30] J. Koshal, A. Nedić and U. V. Shanbhag, "Multiuser optimization: Distributed algorithms and error analysis", *SIAM Journal on Optimization*, Vol. 42, No. 3, pp. 1046-1081, 2011.

APPENDIX

Proof of Theorem IV.4

Proof. Our proof is constructive. We first reduce the Hankel matrix-vector product into an equivalent Toeplitz matrix-vector product and eventually into a Circulant matrix-vector product.

We then show that the last product can be computed efficiently using the Fast Fourier Transform (FFT).

First, we multiply the Hankel matrix $\mathbf{H} \in \mathbb{R}^{n \times m}$ by a matrix $\mathbf{\Pi} \in \mathbb{R}^{m \times m}$ in order to obtain a Toeplitz matrix $\mathbf{T} \in \mathbb{R}^{n \times m}$. The matrix $\mathbf{\Pi}$ is required to have the following structure

$$\mathbf{\Pi} = \begin{pmatrix} 0 & 0 & \cdots & 0 & 1 \\ 0 & 0 & \cdots & 1 & 0 \\ \vdots & & \ddots & & \vdots \\ 1 & 0 & \cdots & 0 & 0 \end{pmatrix}. \quad (25)$$

One can easily verify that indeed

$$\mathbf{H} \cdot \mathbf{\Pi} = \mathbf{T}. \quad (26)$$

Using (26), we can express the product of the Hankel matrix \mathbf{H} with the vector v as

$$\mathbf{H} \cdot v = \mathbf{T} \cdot \mathbf{\Pi}^{-1} \cdot v. \quad (27)$$

One can additionally verify that

$$\mathbf{T} \cdot \mathbf{\Pi} = \mathbf{H}. \quad (28)$$

Thus, we also have that

$$\mathbf{H} \cdot v = \mathbf{T} \cdot \mathbf{\Pi} \cdot v = \mathbf{T} \cdot v_p. \quad (29)$$

where $v_p = \mathbf{\Pi} \cdot v$, $v_p \in \mathbb{R}^m$. This vector has the same elements as v but sorted in reverse order

$$v_p := (v_m \quad v_{m-1} \quad \cdots \quad v_1)^\top. \quad (30)$$

So far we have shown that the product $\mathbf{H} \cdot v$ is equivalent to the product $\mathbf{T} \cdot v_p$. The next step is to embed the Toeplitz matrix \mathbf{T} into a larger Circulant matrix $\mathbf{C} \in \mathbb{R}^{(n+m-1) \times (n+m-1)}$ whose product with a vector can be computed efficiently. We construct the matrix \mathbf{C} as follows

$$\mathbf{C} = \begin{pmatrix} \mathbf{T} & \star \\ \star & \star \end{pmatrix} \quad (31)$$

We emphasize here that, a $n \times m$ Toeplitz matrix \mathbf{T} should be embedded in a $(n+m-1) \times (n+m-1)$ Circulant matrix \mathbf{C} with the matrix \mathbf{T} being on its upper left block. This is because the distinct elements of the $(n+m-1)$ diagonals of the Toeplitz matrix \mathbf{T} are the ones to define the vector c which characterizes the circulant matrix \mathbf{C} and precisely matches its first column. Moving forward, in light of (31), the product $\mathbf{T} \cdot v_p$ can be expressed as a function of the Circulant matrix \mathbf{C} as follows

$$\mathbf{T} \cdot v_p = \begin{pmatrix} I_n & 0_{m-1} \end{pmatrix} \cdot \mathbf{C} \cdot v_e, \quad (32)$$

where the vector v_e is defined as

$$v_e = \begin{pmatrix} v_p \\ 0_{n-1} \end{pmatrix}. \quad (33)$$

We know that the Circulant matrix \mathbf{C} has the nice property of being diagonalized by the Fast Fourier Transform matrix \mathbf{F} . That is,

$$\mathbf{C} = \mathbf{F}^{-1} \mathbf{\Lambda} \mathbf{F}. \quad (34)$$

Hence, the product $\mathbf{C} \cdot v_e$ can be computed as

$$\mathbf{C} \cdot v_e = \mathbf{F}^{-1} \mathbf{\Lambda} \mathbf{F} v_e, \quad (35)$$

which can be written as

$$\mathbf{C} \cdot v_e = \mathbf{F}^{-1} \mathbf{\Lambda} \hat{V}_e, \quad (36)$$

where \hat{V}_e is the Discrete Fourier Transform of v_e and $\mathbf{\Lambda} = \text{diag}(\mathbf{F}c) = \text{diag}(\hat{C})$ is a diagonal matrix with the elements of the discrete fourier transform of the vector c , \hat{C} , on its diagonal. From (32), it is easy to conclude that $\mathbf{H} \cdot v$ can be obtained as the first n elements of the Hadamard product of the vectors \hat{C} and \hat{V}_e . It is important to remember that c is the vector that fully specifies the Circulant matrix \mathbf{C} and corresponds to its first column. That completes the proof. \square

Algorithm 4 can be used to compute efficiently the product p_H of a non-square Hankel matrix $\mathbf{H} \in \mathbb{R}^{n \times m}$ with a vector $v \in \mathbb{R}^m$. In the above analysis, we computed the complexity of the proposed algorithm and proved that it carries out the appropriate computation by exploiting Fast Fourier Transforms (FFT).